

Emergent flux in a one-dimensional Bose-Fermi mixture

Qi Song,¹ Jie Lou,^{1,*} and Yan Chen^{1,†}

¹*Department of Physics and State Key Laboratory of Surface Physics, Fudan University, Shanghai 200433, China*

(Dated: February 7, 2024)

We find a novel chiral superfluid (CSF) phase in a chain of Bose-Fermi mixture, which has been validated using two unbiased numerical methods, density matrix renormalization group and Grassmann multi-scale entanglement renormalization ansatz. The system hosts the interplay between two types of fermions: bare spinless fermions and composite fermions, the latter consisting of a fermion and a boson. In the CSF phase, bosons condensate at non-zero momentum $\pm 2\pi/L$, where L represents the size of the chain. In essence, the local superfluid order parameter continuously rotates along the chain, indicating that the 1D CSF phase spontaneously breaks time-reversal symmetry. This symmetry breaking gives rise to an emergent flux in the background, effectively optimizing the kinetic energy of the composite fermions within the system. We provide a physical understanding at the mean-field level. Furthermore, we demonstrate that the 1D CSF phase can emerge in a more widely applicable extended Hubbard model. The potential realization of this phase in cold-atom experiments has also been explored.

Introduction.— Ultracold atoms loaded into optical lattices provide exceptional platforms for cleanly simulating fundamental theoretical models in condensed matter physics. Over the past two decades, significant advancements have been made in both experimental techniques and theoretical understandings in this field. [1–3] Among them, Bose-Fermi mixtures (BFM)[4–9] aroused significant theoretical and experimental interest. Interactions between fermions and bosons give rise to novel phenomena and new phases. Furthermore, a better understanding of the interplay between these elementary quantum particles may shed light on profound long-term puzzles, such as the origin of high- T_c superconductivity. Considerable effort has been invested in studying one-dimensional BF systems[10–17], which can be experimentally realized by loading alkali atoms into quasi-1D optical lattices with strong transverse confinement. Due to the enhancement of quantum fluctuations in low dimensions, novel physics, such as the formation of composite particles, has been discovered and discussed. Composite particles have also been theoretically discussed [12, 13, 18] and numerically confirmed [14, 17, 19–22] in corresponding models. In these models, onsite neighboring interactions between fermions and bosons play a crucial role. The resulting phase diagram is usually enriched by competitions between multiple interesting quantum phases, including the Luttinger liquid phase of composite particles, a mixed phase featuring coexistence among boson superfluid and fermion liquid, and density-wave states. [23–25].

In this letter, we explore the intricate interplay between bare and composite fermions, focusing on the pivotal role of bosons in this complex system. To capture the essence of this interplay, we introduce a novel model that incorporates the kinetic term of composite fermions (CFs) $-t_{cf}c_i^\dagger b_i^\dagger c_j b_j$. This term replaces the commonly used onsite fermion-boson interaction $U_{bf}n_i^b n_i^f$ in previous studies. [13–25]. Crucially, when a fermion and a

boson bind and hop spontaneously, they gain kinetic energy $-t_{cf}$. This term effectively induces attractive interactions between the two species. Furthermore, we add the free hopping term $-t_f c_i^\dagger c_j$ for the original spinless fermion, destabilizing the composite fermions and introducing competition between spinless fermion and composite fermion, enriching the physics of the system. To enhance the interplay between different particle species, we consider a scenario where the number of fermions (N_f) exceeds the number of bosons (N_b). This ensures that surplus fermions are always present in the mixture, interacting with the composite particles. The resulting Hamiltonian for our system is given by

$$H = -t_f \sum_{\langle ij \rangle} (c_i^\dagger c_j + H.c.) - t_{cf} \sum_{\langle ij \rangle} (c_i^\dagger b_i^\dagger c_j b_j + H.c.) + \frac{U_{bb}}{2} \sum_i n_i^b (n_i^b - 1) - \mu_b \sum_i n_i^b - \mu_f \sum_i n_i^f \quad (1)$$

where U_{bb} represents the onsite repulsive interaction between bosons, $n_i^b(n_i^f)$ is the onsite boson (fermion) number operator, and $\mu_b(\mu_f)$ is the chemical potential of bosons (fermions).

Emergence of Flux State.— We employ both the density matrix renormalization group (DMRG)[26, 27] and Grassmann multi-scale entanglement renormalization ansatz (GMERA)[28] methods, two well-established unbiased numerical techniques based on tensor product ansatz, to study this BFM model.[29] Our calculations reveal an intriguing outcome: due to strong scattering interactions, when $t_{cf} < t_f$, bosons decouple from composite particles and enter a superfluid state. More remarkably, when the number of fermions N_f in the system is even, the bosons condense at non-zero momentum $k_0 = \pm 2\pi/L$, where L represents the size of the periodic chain (Fig. 3). In contrast to conventional superfluids, where condensation occurs at $k = 0$, this non-zero momentum condensation leads to a complex local order

parameter $\langle b_i \rangle$ that rotates continuously along the chain. The twisted angles θ_{ij} (argument difference between $\langle b_i \rangle$ and $\langle b_j \rangle$ on two neighboring sites (i, j)) add up to 2π over a complete lattice period, as illustrated in Fig. 1. This chiral superfluid (CSF) state spontaneously breaks time-reversal symmetry, resulting in a unique and intriguing emergent flux state in the Bose-Fermi mixture.

Origin of CSF.— Here we approach the origin of CSF from two distinct perspectives, starting from the bare fermion limit ($t_f \gg t_{cf}$). First, the kinetic term of composite particles (t_{cf}) suggests that a bosonic superfluid in the background induces projected "silhouette" composite particles, favoring an energy-optimized state. A CSF introduces an additional phase factor that fermions acquire during hopping. Effectively, this generates an "emergent flux" that further improves the system energy, analogous to the behavior of electrons hopping in a ring with a magnetic flux[30]. Based on this argument, we develop a mean-field consideration, resulting in an effective boson-free model that qualitatively aligns with our original Hamiltonian in the bare fermion limit.

Second, the fermionic response to the bosonic emergent flux is crucial. As the CSF emerges, it profoundly modifies the fermionic momentum distribution. Numerical calculations reveal that the degeneracy of the fermionic Fermi surface (two Fermi points) is lifted simultaneously when the time-reversal symmetry of the superfluid is broken. This lifting of degeneracy is accompanied by a redistribution of the momentum distribution of composite particles, which becomes more concentrated around small k values, further optimizing the system's energy. The collaborative effect between the fermionic and bosonic sectors is crucial in stabilizing the CSF state.

We want to emphasize that the CSF phase is not merely an artifact of the composite hopping term; instead, it naturally arises within a standard Bose-Fermi mixed Hubbard model with extended nearest-neighbor interactions. This finding significantly enhances the feasibility of experimentally realizing one-dimensional CSF in optical lattices. Furthermore, our system exhibits an intriguing sensitivity to the parity of fermions. Specifically, when the number of fermions N_f is even, the bosonic superfluid (SF) manifests chirality. However, when N_f is odd, the SF reverts to its conventional form. This parity-dependent chirality suggests that the chirality of this quantum system, protected by an energy gap, can be controlled by simply adding or removing particles through tuning chemical potentials. Such controllable chirality has implications for quantum computation. In the latter part of this paper, we will present numerical evidence to support our claims and discuss possible experimental setups for realizing and probing this CSF phase.

To better understand the origin of the CSF, it is enlightening to explore the fundamental differences between systems with even and odd number of fermions (N_f). When N_f is odd, bosons condensate at $k = 0$, similar

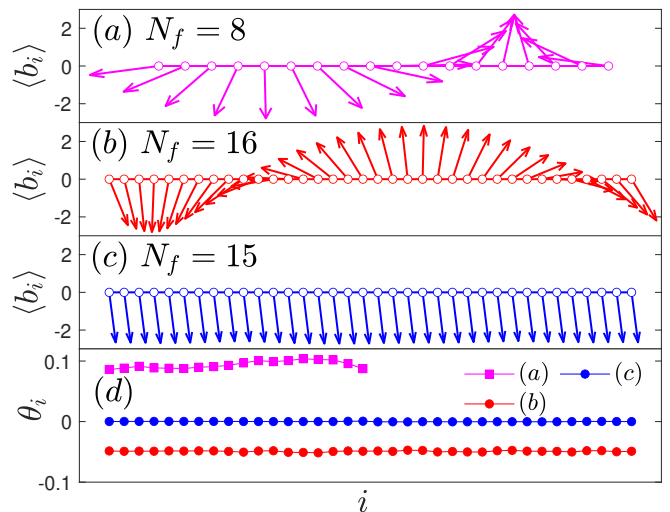


FIG. 1. (a)–(c): The boson superfluid order parameter $\langle b_i \rangle$ (arrows) measured on each site i (open circles), magnified 10 times, with horizontal/vertical component of the arrow corresponding to its real/imaginary part, respectively. (d): The argument angle θ_i of the nearest-neighbor hopping term $\langle b_i^\dagger b_{i+1} \rangle$. Results are obtained at parameter setting $t_f = 0.2, t_{cf} = 0.4, U_{bb} = 3.0$.

to a conventional superfluid. In contrast, when N_f is even, the ground state is in the CSF phase where bosons condensate at $k_0 = \pm 2\pi/L$, either clockwise or counter-clockwise, depending on the sign of k_0 .

In both cases, the SF phase persists to an intense competition region $t_f \approx t_{cf}$. To gain further understanding, we start from the free bare fermion limit, where $t_f \gg t_{cf}$. Numerical results show that superfluidity emerges as soon as t_{cf} is turned on, such as ($t_{cf} = 10^{-3}t_f$). This is confirmed by the results of long-range boson correlation $G_b(x) = \langle b_i^\dagger b_{i+x} \rangle$ and momentum distribution $n_b(k)$ from both DMRG and GMERA calculations. This observation can be understood from the uncorrelated scenario, where boson and fermion do not interact. In this case, with a boson superfluid in the background, free hopping fermions can gain additional energy through the t_{cf} term in Eqn. 1, by projecting out silhouette composite particles. In another word, for a conventional SF (N_f is odd), contribution from composite particle hopping $c_i^\dagger c_j b_i^\dagger b_j$ in this limit can simply be considered as $c_i^\dagger c_j \langle b \rangle^2$ where $\langle b \rangle$ is the uniform superfluid amplitude, and it is available as long as $\langle b \rangle$ is non-zero.

When N_f is even, the energy contribution from the t_{cf} term can be further improved by allowing superfluid order parameter $\langle b \rangle$ to rotate and acquire chirality. In such cases, the hopping amplitude $\langle b_i^\dagger b_j \rangle$ becomes a complex number due to the phase difference of $\langle b \rangle$ between neighboring sites. Consequently, the expression $c_i^\dagger c_j b_i^\dagger b_j$ should be regarded as $c_i^\dagger c_j \langle b_i^\dagger b_j \rangle$. Numerical results confirm that the measurement of $\langle b_i^\dagger b_j \rangle$ on different bond

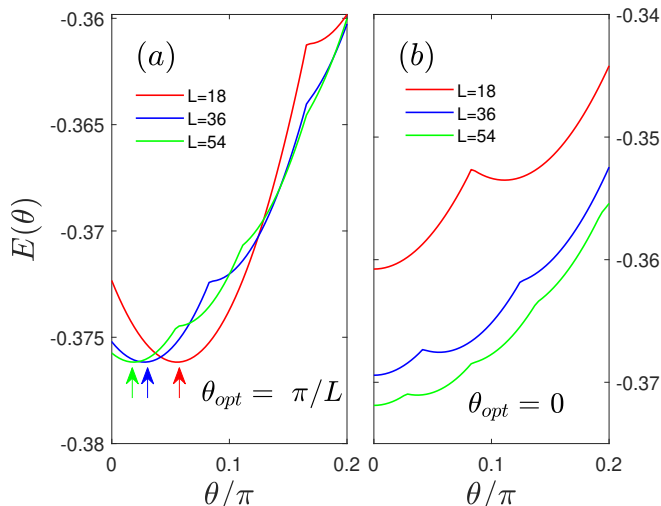


FIG. 2. The ground state energy $E(\theta)$ of the mean-field Hamiltonian H_{MF} as a function of the argument θ in $L = 18, 36, 54$ systems when $t_f = 0.2, t_{cf} = 0.4$. (a) Even fermion parity. Fermion filling factor is fixed at $n_f = N_f/L = 4/9$. There is a prominent peak on $\theta = 0$ where no magnetic flux is threaded through the system. And $E(\theta)$ reaches its absolute minimum at $\theta_{opt} = \pi/L$. (b) Odd fermion parity. N_f are 7, 15, 23 for $L = 18, 36, 54$ respectively. No peak shows on $\theta = 0$ contrary to the even case in the main panel. And $E(\theta)$ reaches its absolute minimum at $\theta_{opt} = 0$

$\langle i, j \rangle$ exhibit nearly identical arguments and moduli, as shown in Fig. 1(d). This observation suggests that a CSF generates an additional phase factor $e^{i\theta_{ij}}$ in the composite hopping term.

Explanation from effective flux.— This enlighten us to trace back to the "flux phase" problem [31–34] which provides insight into why magnetic flux can lower the ground-state energy of fermions. Extensive studies have shown that the energy of electrons can be significantly improved by the presence of magnetic flux penetrating the lattice, both in one-dimensional (1D) systems [35] and in higher dimensions [36–38]. In the specific case of spinless fermions in 1D, rigorous theoretical works [39–41] have established that the optimal total flux phase $\Phi = \pi$ when N_f is even, 0 otherwise.

Next we apply a mean-field approximation to our Hamiltonian (1) to acquire a corresponding boson-free mean-field level model

$$H_{MF} = -t_f \sum_{\langle ij \rangle} (c_i^\dagger c_j + H.c.) - t'_{cf} \sum_{\langle ij \rangle} (c_i^\dagger c_j e^{i\theta} + H.c.) \quad (2)$$

where the influence of bosons has been classically treated as a pure phase factor $e^{i\theta}$ attached to each spinless fermion hopping term. It is understood that tight-binding electrons enter a flux phase $\theta = \theta_{\langle ij \rangle} = 2\pi \int_i^j \mathbf{A} \cdot d\mathbf{l}$ in the presence of a magnetic field on a lattice structure, where \mathbf{A} is the vector potential [30]. When a

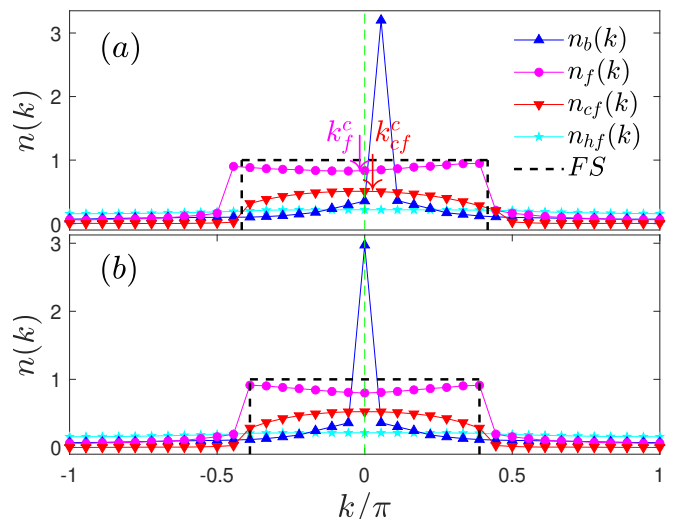


FIG. 3. Momentum distribution functions $n(k)$ for $L = 36$ system with boson filling factor $n_b \approx 1/4$, obtained by GMERA. "FS" refers to the symmetric Fermi surface of original fermions. (a) For $N_f = 16$, an even number, bosons condensate at $|k_0| = 2\pi/L$ (position of the blue peak in $n_b(k)$). $k_f^c = \sum_k n_f(k) \times k/N_f = -0.0122\pi$ is the center of original fermion sea, whereas $k_{cf}^c = \sum_k n_{cf}(k) \times k/N_{cf} = 0.0075\pi$ is the center of fermi sea for composite fermion, where $N_{cf} = \sum_k n_{cf}(k)$. (b) For $N_f = 15$ (odd), bosons condensate at $k = 0$. Results are obtained at parameter setting $t_f = 0.2, t_{cf} = 0.4, U_{bb} = 3.0$. Fourier transforms of $G_b(i, j) = \langle b_i^\dagger b_j \rangle$, $G_f(i, j) = \langle c_i^\dagger c_j \rangle$, $G_{cf}(i, j) = \langle c_i^\dagger b_i^\dagger c_j b_j \rangle$ and $G_{hf}(i, j) = \langle c_i^\dagger b_i c_j b_j^\dagger \rangle$ give respective momentum distributions $n_b(k), n_f(k), n_{cf}(k)$ and $n_{hf}(k)$. The green dashed lines guide the eyes at $k = 0$.

fermion moves around a ring, it experiences total magnetic flux $\Phi = \sum_{i=1}^L \theta_{\langle ij \rangle} = L\theta$. Thus, the mean-field Hamiltonian H_{MF} reflects the competition between two hopping terms: the former stands for original free hopping, whereas the latter expresses hoppings experiencing a lattice flux.

This model can be solved straightforwardly. As shown in Fig. 2, the ground state energy E exhibits a periodically varying function superimposed on a parabolic background. This shape reveals the competition between two distinct hopping processes. In other words, $c_i^\dagger c_j$ also breaks time-reversal symmetry under the influence of flux. Remarkably, a significant difference is observed between systems with even (left panel) and odd (right panel) fermion parity: when N_f is even, the optimal θ equals to π/L , a non-zero value. In contrast, when N_f is odd, the energy is optimized when θ takes the value of 0.

This observation from the mean-field model is similar to the results obtained in the BFM. However, it is crucial to note that the flux phase θ_{ij} , namely the argument of the complex $\langle b_i^\dagger b_{i+1} \rangle$ shown in Fig. 1(d), averages out to 0.0940π for $L = 18$ or -0.0491π for $L = 36$, deviating from the optimal angle of π/L predicted by mean-

field theory. This deviation is attributed to the periodic boundary conditions imposed on our homogeneous lattice. Nevertheless, the ground-state energy has been optimized as the CSF phase becomes the ground-state.

As stated above, our findings indicate that the motions of bare fermions break time-reversal symmetry under the influence of the effective boson 'flux.' To further corroborate this, we introduce a counter-hopping term $-t_{hf}c_i^\dagger b_i c_{i+1} b_{i+1}^\dagger$, with an amplitude t_{hf} equal to t_{cf} . Numerical results show that the new ground state exhibits uniform superfluid order $\langle b_i \rangle$ with equivalent modulus on each site i , regardless of fermion parity. This can be intuitively understood through our mean-field ansatz, where counter hopping is replaced by $c_i^\dagger c_j e^{-i\theta}$. When both t_{cf} and t_{hf} terms are considered, they combine as $c_i^\dagger c_j e^{i\theta} + c_i^\dagger c_j e^{-i\theta} = 2c_i^\dagger c_j \cos(\theta)$, thereby naturally favoring uniform superfluidity in terms of energy.

The shift of Fermi surface.— Interplay and correlations between different species of particles lead to the shift of the Fermi surface. We focus on the correlation function and momentum distribution of involved particles, influenced by the effective flux. When N_f is odd, the conventional bosonic superfluid can be considered as a flux-free background, the correlation function of projected composite fermion $G_{cf}(i, j) = \langle c_i^\dagger b_i^\dagger c_j b_j \rangle$ shows similar long-range behavior as that of an original fermion. As demonstrated in Fig. 3, two clear Fermi surfaces (points) of composite particles have the same momentum as those of spinless fermions. Contrastingly, when N_f is even, the ground state exhibits a two-fold degeneracy: bosons condensate at either $+2\pi/L$ or $-2\pi/L$, time-reversal symmetry of the system is spontaneously broken. Intriguingly, this degeneracy lift simultaneously affects the Fermi surface of a bare fermion. The selection of the last filled momentum is determined by the direction of the effective flux, resulting in an asymmetric bulk of the Fermi Sea. Consequently, the Fermi sea of the projected composite fermion shifts towards $k = 0$, optimizing the system's overall energy. In this uncorrelated limit, this projection can be rationalized as follows:

$$\begin{aligned} n_{cf}(k) &= 1/L \sum_{i,j} G_{cf}(i, j) e^{ik(x_i - x_j)} \\ &\approx 1/L \sum_{i,j} G_f(i, j) G_b(i, j) e^{ik(x_i - x_j)} \\ &\approx 1/L \sum_{i,j} G_f(i, j) |A| e^{i(k+k_0)(x_i - x_j)} \quad (3) \end{aligned}$$

Here, $G_b(i, j) = |A| e^{ik_0(x_i - x_j)}$ represents the boson correlation for superfluid condensates at momentum k_0 .

By carefully comparing DMRG and GMERA results, we confirm that the CSF order is energetically favorable. In Fig. 3, we present the momentum distribution derived from GMERA calculations. DMRG calculations often maintain degeneracy and symmetry, as evident in Fig. 5.

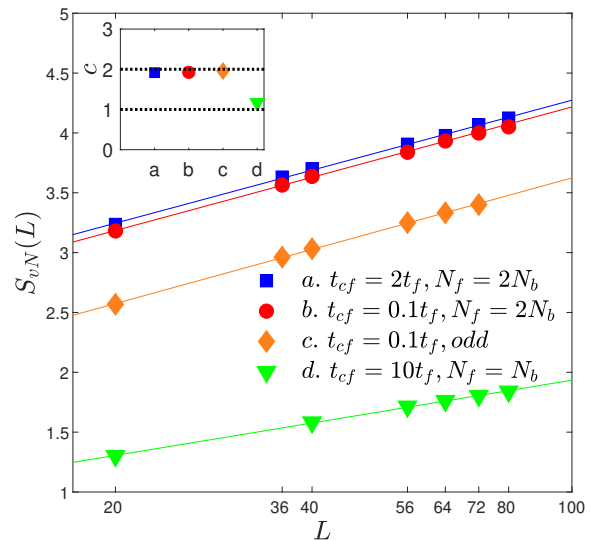


FIG. 4. The entanglement entropy S_{vN} as a function of L at different values of t_{cf}/t_f and fermion parity. Boson and fermion numbers are $N_f = N_b = L/2$ in 'a' (blue solid squares) and 'b' (red solid circles), $N_f = L/2 - 1$, $N_b = L/2$ in 'c' (orange solid diamonds) and $N_f = N_b = L/2$ in 'd' (green solid triangles). Inset: The central charge corresponding to the fitting lines of 'a', 'b', 'c', and 'd'.

Conversely, GMERA outcomes are prone to symmetry-breaking. Please refer to the Supplementary Material [29] for further details.

We must clarify that the Fermi surface of the projected CF is not precisely centered at $k = 0$ and exhibits an asymmetric shape. The optimal condensation momentum k that we can achieve is restricted to $k_0 = 2\pi/L$ (which is larger than the ideal value of π/L) due to the periodic boundary conditions of our homogeneous lattice, as previously explained.

Comments about strong correlations.— Although the previous explanation is based on the uncorrelated limit, which serves as a flux background, the CSF phase remains remarkably stable up to $t_f \approx t_{cf}$. A noteworthy difference emerges between $\langle c_i^\dagger b_i^\dagger c_{i+1} b_{i+1} \rangle$ and $\langle c_i^\dagger b_i c_{i+1} b_{i+1}^\dagger \rangle$ that grows as t_{cf} increases. This distinction suggests a deviation from the uncorrelated scenario since a straightforward uncorrelated superfluid background fails to distinguish between these two terms. Additional evidence can be found in the momentum distribution $n(k)$ of the intermediate region. The singularity of the Fermi surface for spinless fermions and composite particles is significantly altered by strong correlations, manifesting as convex and concave features in $n(k)$ near $k = 0$ due to strong scattering.

Intriguingly, the central charge obtained from entanglement entropy in DMRG calculations remains consistently ≈ 2 , as illustrated in Fig. 4. This observation indicates that, despite the projected particle's contribu-

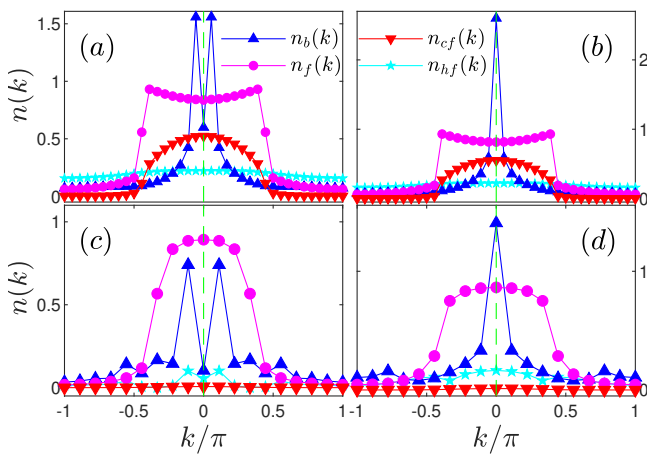


FIG. 5. Momentum distribution functions $n(k)$ obtained by DMRG. (a) $N_f = 16 = 2N_b$ and (b) $N_f = 15, N_b = 8$ correspond to the Hamiltonian (1) at $t_{cf} = 2t_f = 0.4$ for $L = 36$ sites. (c) $N_f = 6, N_b = 3$ and (d) $N_f = 7, N_b = 4$ correspond to the extended BF Hamiltonian (4) at $t_f = 0.4, t_b = 0.05, U_{bb} = 3.0, U_{bf} = 3.0, V_{bf} = -0.3$ for $L = 18$ sites. For even N_f (Left column), bosons condensate at $|k_0| = 2\pi/L$ (positions of the two blue peaks in $n_b(k)$). For odd N_f (right column), bosons condensate at $k = 0$.

tion to optimizing the system's total energy, it resembles the original particles. Global excitations are contributed by bosons (in superfluidity) and fermions (Luttinger liquid).

It is worth mentioning that the condensation of a bosonic superfluid at a momentum $k \neq 0$ has been previously explored in various works, including those studying systems with correlated hopping [42, 43], as well as in the experimental realization of a two-dimensional topological chiral superfluid observed in optical lattice experiments [44–46]. Nevertheless, the microscopic origin of the one-dimensional CSF in our system is fundamentally different. It arises directly from the interplay between two species of fermions and serves as a background field to optimize the system's overall energy.

CSF in Extended Bose-Fermi model.— We have elucidated the origin of the 1D CSF phase using a model that incorporates the kinetic energy of composite fermions. However, this seemingly “artificial” term is not an indispensable component. Indeed, the 1D CSF phase can be derived from the extended Hubbard model, which is given by

$$\begin{aligned}
 H_{BF} = & - \sum_{\langle ij \rangle} (t_f c_i^\dagger c_j + t_b b_i^\dagger b_j + H.c.) \\
 & + \frac{U_{bb}}{2} \sum_i n_i^b (n_i^b - 1) + U_{bf} \sum_i n_i^b n_i^f \\
 & + V_{bf} \sum_{\langle ij \rangle} (n_i^b n_j^f + n_i^f n_j^b) / 2.
 \end{aligned} \quad (4)$$

where t_b represents the hopping amplitude of bosons,

while $t_f, U_{bb}, n_i^b, n_i^f$ retain the same meanings as in Hamiltonian (1).

In the standard BF Hubbard model, we introduce an asymmetry by setting an unequal number of bosons and fermions. This asymmetry leads to strong scattering of composite particles by surplus fermions, resulting in instability. The Hamiltonian incorporates a standard on-site boson-fermion repulsion term U_{bf} [17], facilitating the formation of composite particles. Additionally, a nearest-neighbor attraction V_{bf} is introduced to prevent phase separation or collapse of particles. The filling factor of fermion is less than $1/3$ to avoid collapse state[19] and $N_f \approx 2N_b$. When $t_f \approx 10t_b$ and U_{bf} is one order larger than t_f ($U_{bf} = U_{bb}$), DMRG simulations show that bosons condensate at $|k_0| = 2\pi/L$ with even fermion number N_f , as shown in Fig. 5(c) similar to that in Fig. 5(a). For odd N_f in Fig. 5(d), bosons condensate at $k = 0$ similar to that in Fig. 5(b). This even-odd difference is concrete evidence that obtaining the CSF phase in the extended BF Hubbard model is possible. Simulating this phase is more feasible in experimental settings than with the Hamiltonian given by Eq. (1).

Discussion.— Our study reveals a novel many-body effect in a 1D BFM system where the CSF phase emerges and breaks TSR spontaneously to optimize the energy of the whole system. With the thriving development of quantum simulation experiments[1–3, 47], our model promises to be effectively simulated in an optical lattice utilizing a combination of ultracold bosonic and fermionic atoms[48–51]. Experimentally, periodic boundary conditions have been achieved in a 1D ring-shaped optical lattice with finite sites.[52–56] The characteristic signature of the CSF phase can be observed through widely utilized time-of-flight (TOF) experiments, which restore phase coherence information throughout the entire lattice[1, 57]. The density distribution captured in TOF images corresponds to the momentum distribution of the trapped atoms. During TOF expansion, the fermionic atoms influenced by an effective flux induced by the bosonic CSF will exhibit a doughnut-shaped pattern (analogous to the right panel of FIG.5 in Ref.[56]). This pattern contrasts with the bell-shaped pattern observed when bosons are in a normal superfluid state and fermions experience no effective flux [56].

ACKNOWLEDGEMENTS

This work is supported by the National Key Research and Development Program of China Grant No. 2022YFA1404204, and the National Natural Science Foundation of China Grant No. 12274086.

-
- * loujie@fudan.edu.cn
† yanchen99@fudan.edu.cn
- [1] I. Bloch, J. Dalibard, and W. Zwerger, *Rev. Mod. Phys.* **80**, 885 (2008).
 - [2] C. Gross and I. Bloch, *Science* **357**, 995 (2017).
 - [3] F. Schfer, T. Fukuhara, S. Sugawa, Y. Takasu, and Y. Takahashi, *Nature Reviews Physics* **2**, 411 (2020).
 - [4] M. Lewenstein, A. Sanpera, V. Ahufinger, B. Damski, A. Sen(De), and U. Sen, *Advances in Physics* **56**, 243 (2007).
 - [5] X.-W. Guan, M. T. Batchelor, and C. Lee, *Rev. Mod. Phys.* **85**, 1633 (2013).
 - [6] J. J. Kinnunen, Z. Wu, and G. M. Bruun, *Phys. Rev. Lett.* **121**, 253402 (2018).
 - [7] F. Ferlaino, E. de Mirandes, G. Roati, G. Modugno, and M. Inguscio, *Phys. Rev. Lett.* **92**, 140405 (2004).
 - [8] I. Ferrier-Barbut, M. Delehaye, S. Laurent, A. T. Grier, M. Pierce, B. S. Rem, F. Chevy, and C. Salomon, *Science* **345**, 1035 (2014).
 - [9] B. J. DeSalvo, K. Patel, G. Cai, and C. Chin, *Nature* **568**, 61 (2019).
 - [10] M. A. Cazalilla and A. F. Ho, *Phys. Rev. Lett.* **91**, 150403 (2003).
 - [11] E. Orignac, M. Tsuchiizu, and Y. Suzumura, *Phys. Rev. A* **81**, 053626 (2010).
 - [12] A. Imambekov and E. Demler, *Phys. Rev. A* **73**, 021602 (2006).
 - [13] X. Barillier-Pertuisel, S. Pittel, L. Pollet, and P. Schuck, *Phys. Rev. A* **77**, 012115 (2008).
 - [14] A. Mering and M. Fleischhauer, *Phys. Rev. A* **77**, 023601 (2008).
 - [15] C. N. Varney, V. G. Rousseau, and R. T. Scalettar, *Phys. Rev. A* **77**, 041608 (2008).
 - [16] L. Mathey, D.-W. Wang, W. Hofstetter, M. D. Lukin, and E. Demler, *Phys. Rev. Lett.* **93**, 120404 (2004).
 - [17] L. Pollet, M. Troyer, K. Van Houcke, and S. M. A. Rombouts, *Phys. Rev. Lett.* **96**, 190402 (2006).
 - [18] M. Lewenstein, L. Santos, M. A. Baranov, and H. Fehrmann, *Phys. Rev. Lett.* **92**, 050401 (2004).
 - [19] M. Rizzi and A. Imambekov, *Phys. Rev. A* **77**, 023621 (2008).
 - [20] I. Danshita and L. Mathey, *Phys. Rev. A* **87**, 021603 (2013).
 - [21] P. Anders, P. Werner, M. Troyer, M. Sgrist, and L. Pollet, *Phys. Rev. Lett.* **109**, 206401 (2012).
 - [22] L. Pollet, C. Kollath, U. Schollwöck, and M. Troyer, *Phys. Rev. A* **77**, 023608 (2008).
 - [23] H. P. Büchler and G. Blatter, *Phys. Rev. Lett.* **91**, 130404 (2003).
 - [24] F. Hébert, G. G. Batrouni, X. Roy, and V. G. Rousseau, *Phys. Rev. B* **78**, 184505 (2008).
 - [25] I. Titvinidze, M. Snoek, and W. Hofstetter, *Phys. Rev. Lett.* **100**, 100401 (2008).
 - [26] S. R. White, *Phys. Rev. Lett.* **69**, 2863 (1992).
 - [27] ITENSOR, <http://itensor.org>.
 - [28] J. Lou and Y. Chen, (2015), [arXiv:1506.03716](https://arxiv.org/abs/1506.03716).
 - [29] See supplementary materials.
 - [30] D. Peter, M. Cyrot, D. Mayou, and S. N. Khanna, *Phys. Rev. B* **40**, 9382 (1989).
 - [31] P. Wiegmann, *Physica C: Superconductivity* **153-155**, 103 (1988).
 - [32] E. H. Lieb, *Helvetica Physica Acta* **65**, 247 (1992).
 - [33] E. Lieb and M. Loss, *Duke Mathematical Journal* **71**, 337 (1993).
 - [34] N. Macris and B. Nachtergaele, *Journal of Statistical Physics* **85**, 745 (1996).
 - [35] F. Nakano, *Journal of Physics A: Mathematical and General* **33**, 5429 (2000).
 - [36] Y. Hasegawa, P. Lederer, T. M. Rice, and P. B. Wiegmann, *Phys. Rev. Lett.* **63**, 907 (1989).
 - [37] Y. Hasegawa, Y. Hatsugai, M. Kohmoto, and G. Montambaux, *Phys. Rev. B* **41**, 9174 (1990).
 - [38] E. H. Lieb, *Phys. Rev. Lett.* **73**, 2158 (1994).
 - [39] W. Nie, H. Katsura, and M. Oshikawa, *Phys. Rev. Lett.* **111**, 100402 (2013).
 - [40] W. Nie, H. Katsura, and M. Oshikawa, *Phys. Rev. B* **97**, 125153 (2018).
 - [41] W. Zheng, *Journal of Statistical Mechanics: Theory and Experiment* **2020**, 073103 (2020).
 - [42] J. Struck, C. Ölschläger, M. Weinberg, P. Hauke, J. Simonet, A. Eckardt, M. Lewenstein, K. Sengstock, and P. Windpassinger, *Phys. Rev. Lett.* **108**, 225304 (2012).
 - [43] T. Keilmann, S. A. Lanzmich, I. McCulloch, and M. Roncaglia, *Nature communications* **2**, 361 (2010).
 - [44] X.-Q. Wang, G.-Q. Luo, J.-Y. Liu, W. V. Liu, A. Hemmerich, and Z.-F. Xu, *Nature* **596**, 227 (2021).
 - [45] T. Kock, M. Ölschläger, A. Ewerbeck, W.-M. Huang, L. Mathey, and A. Hemmerich, *Phys. Rev. Lett.* **114**, 115301 (2015).
 - [46] P. Soltan-Panahi, D.-S. Lühmann, J. Struck, P. Windpassinger, and K. Sengstock, *Nature Physics* **8**, 71 (2012).
 - [47] C. Weitenberg and J. Simonet, *Nature Physics* **17**, 1342 (2021).
 - [48] A. G. Truscott, K. E. Strecker, W. I. McAlexander, G. B. Partridge, and R. G. Hulet, *Science* **291**, 2570 (2001).
 - [49] C. A. Stan, M. W. Zwierlein, C. H. Schunck, S. M. F. Raupach, and W. Ketterle, *Phys. Rev. Lett.* **93**, 143001 (2004).
 - [50] S. Inouye, J. Goldwin, M. L. Olsen, C. Ticknor, J. L. Bohn, and D. S. Jin, *Phys. Rev. Lett.* **93**, 183201 (2004).
 - [51] T. Fukuhara, S. Sugawa, Y. Takasu, and Y. Takahashi, *Phys. Rev. A* **79**, 021601 (2009).
 - [52] S. Franke-Arnold, J. Leach, M. J. Padgett, V. E. Lembessis, D. Ellinas, A. J. Wright, J. M. Girkin, P. Öhberg, and A. S. Arnold, *Optics Express* **15**, 8619 (2007).
 - [53] L. Amico, A. Osterloh, and F. Cataliotti, *Phys. Rev. Lett.* **95**, 063201 (2005).
 - [54] N. Houston, E. Riis, and A. S. Arnold, *Journal of Physics B: Atomic, Molecular and Optical Physics* **41**, 211001 (2008).
 - [55] L. Amico, D. Aghamalyan, F. Auksztol, H. Crepaz, R. Dumke, and L. C. Kwek, *Scientific Reports* **4**, 4298 (2014).
 - [56] L. Amico, D. Anderson, M. Boshier, J.-P. Brantut, L.-C. Kwek, A. Minguzzi, and W. von Klitzing, *Rev. Mod. Phys.* **94**, 041001 (2022).
 - [57] M. Greiner, O. Mandel, T. Esslinger, T. W. Hnsch, and I. Bloch, *Nature* **415**, 39 (2002).